AD-A205 962

A NUMERICAL MODEL OF THE EFFECTS OF PROPELLER WASH AND SHIP-INDUCED WAVES FROM COMMERCIAL NAVIGATION IN AN EXTENDED NAVIGATION SEASON ON EROSION, SEDIMENTATION, AND WATER QUALITY IN THE GREAT LAKES CONNECTING CHANNELS AND HARBORS

DTIC
SELECTE
MAR 0 3 1989
S D
D

Prepared for

U.S. Army Corps of Engineers
Detroit District

by

Anatoly B. Hochstein and Charles E. Adams, Jr.

Baton Rouge, Louisiana

September 1986

89 12 29 0[illegible]

Unclassified

SECURITY CLASSIFICATION OF THIS PAGE

REPORT DOCUMENTATION PAGE

Form Approved OMB No. 0704-0188

1a. REPORT SECURITY CLASSIFICATION: Unclassified	1b. RESTRICTIVE MARKINGS
2a. SECURITY CLASSIFICATION AUTHORITY	3. DISTRIBUTION/AVAILABILITY OF REPORT: Approved for public release; distribution unlimited
2b. DECLASSIFICATION/DOWNGRADING SCHEDULE	
4. PERFORMING ORGANIZATION REPORT NUMBER(S): None	5. MONITORING ORGANIZATION REPORT NUMBER(S)
6a. NAME OF PERFORMING ORGANIZATION: Hochstein, A.B., and C.E. Adams, Jr. / 6b. OFFICE SYMBOL (If applicable)	7a. NAME OF MONITORING ORGANIZATION: U.S. Army Corps of Engineers
6c. ADDRESS (City, State, and ZIP Code): Baton Rouge, Louisiana	7b. ADDRESS (City, State, and ZIP Code): Detroit District, P.O. Box 1027, Detroit, MI 48231
8a. NAME OF FUNDING/SPONSORING ORGANIZATION: U.S. Army Corps of Engineers / 8b. OFFICE SYMBOL (If applicable)	9. PROCUREMENT INSTRUMENT IDENTIFICATION NUMBER: DACW35-85-C-0064
8c. ADDRESS (City, State, and ZIP Code): Detroit District, P.O. Box 1027, Detroit, MI 48231	10. SOURCE OF FUNDING NUMBERS: PROGRAM ELEMENT NO. / PROJECT NO / TASK NO / WORK UNIT ACCESSION NO

11. TITLE (Include Security Classification)

A Numerical Model of the Effects of Propeller Wash and Ship-Induced Waves from Commercial Navigation in an Extended Navigation Season on Erosion.

12. PERSONAL AUTHOR(S)

Hochstein, A.B., and C.E. Adams, Jr.

13a. TYPE OF REPORT	13b. TIME COVERED	14. DATE OF REPORT (Year, Month, Day)	15. PAGE COUNT
Final	FROM _____ TO _____	September 1986	47

16. SUPPLEMENTARY NOTATION

17. COSATI CODES			18. SUBJECT TERMS (Continue on reverse if necessary and identify by block number)
FIELD	GROUP	SUB-GROUP	Mathematical Model, FORTRAN 77, IBM-PC-AT, Propeller Wash, Ship-Induces Waves, Erosion, Suspended Solids, Extended Season

19. ABSTRACT (Continue on reverse if necessary and identify by block number)

Forces generated over and above the natural forces created by fluid flow in channels stems from ship traffic in river channels. When the magnitude is sufficient, these forces can have an adverse impact on the natural river flow environment. Propeller jet and displacement or backwater flow velocities, ship waves and "drawdown" effects all contribute in part to development of these forces. In order to plan for improvement and optimum use of waterways, it is necessary to estimate the magnitude of these forces and the resulting environmental effects, especially channel bed erosion rates and the increase of suspended solids. This report addresses the effects of propeller jet and backwater velocities and ship-induced waves by creating a mathematical model. Predictive equations based on a combination of theory and observations have been developed for estimating the unknown quantities. Equations are

20. DISTRIBUTION/AVAILABILITY OF ABSTRACT: ☒ UNCLASSIFIED/UNLIMITED ☐ SAME AS RPT ☐ DTIC USERS	21. ABSTRACT SECURITY CLASSIFICATION: Unclassified
22a. NAME OF RESPONSIBLE INDIVIDUAL: Thomas Freitag	22b. TELEPHONE (Include Area Code): (313) 226-7590 / 22c. OFFICE SYMBOL: CENCE-PD-EA

DD Form 1473, JUN 86 *Previous editions are obsolete.* SECURITY CLASSIFICATION OF THIS PAGE

#11 (cont.) Sedimentation, and Water Quality in the Great Lakes Connecting Channels and Harbors

#19 (cont.) used to model forces created by vessels transiting harbors and connecting channels of the Great Lakes. The mathematical model has been computerized in FORTRAN 77 code for real-time execution on an IBM-PC-AT computer or compatible machine with at least 10 mcgabytes of random access memory. The principal objective of the computer model is to permit an assessment of the environmental effects of vessel operation in an extended navigation season when ice cover is present.

CONTENTS

ILLUSTRATIONS

TABLES

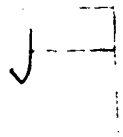

A-1

A NUMERICAL MODEL OF THE EFFECTS OF PROPELLER WASH AND SHIP-INDUCED WAVES FROM COMMERCIAL NAVIGATION IN AN EXTENDED NAVIGATION SEASON ON EROSION, SEDIMENTATION, AND WATER QUALITY IN THE GREAT LAKES CONNECTING CHANNELS AND HARBORS

INTRODUCTION

Ship traffic in river channels generates forces over and above the natural forces created by fluid flow in the channel that, when of a sufficient magnitude, can have an adverse impact on the natural fluvial environment. These forces are developed, in part, as a result of propeller jet and displacement or backwater flow velocities. Other important forces are ship waves and so-called "drawdown" effects. All of these forces interfere although some are strong functions of channel section, vessel speed, etc. Estimation of the magnitudes of these forces and their resulting environmental effects, principally channel bed erosion rates and the increase of suspended solids, is an important element in the development of plans for improvement and optimum utilization of waterways. The following presentation encompasses the effects of propeller jet and backwater velocities and ship-induced waves.

Predictive equations based on a combination of theory and observations have been developed for estimating the unknown quantities. The equations are used to model forces created by vessels transiting harbors and interconnecting channels of the Great Lakes. The mathematical model has been computerized in FORTRAN 77 code for real-time execution on an IBM PC-AT computer or a compatible machine with at least 10 megabytes of random access memory. A principal objective of the computer model is to permit an assessment of the environmental effects of vessel operations in an extended navigation season when ice cover is present. Example results are presented for two locations on the St. Marys River. While the model has been calibrated for the St. Marys River, it is sufficiently general to be of use in other similar geographic and environmental settings.

ENVIRONMENTAL SETTING

The St. Marys River, an important commercial navigation artery, connects Lake Superior and Lake Huron along the border between the United States (Michigan) and Canada (Ontario). Water elevation drops about 22 feet along the 60 mile length of the river. Much of the elevation difference occurs at the St. Marys Falls which are negotiated by ships in one step via a set of parallel locks. The river consists of a succession of natural and man-made channel sections which exhibit a variety of physical and natural characteristics and dimensions. In winter the St. Marys River accumulates an extensive cover of ice.

Several lines of evidence suggest that propwash from commercial vessel passages causes a disturbance of St. Marys River channel sediments. The evidence includes observations of increased turbidity and suspended-sediment concentrations following vessel transits as well as a paucity of benthic organisms on the channel bed in some areas, which may not be due to substrate or temperature differences. Disturbance of channel sediments may be enhanced during the winter season when navigation in ice requires the use of increased vessel power.

The extent and intensity of disturbance of bottom sediments is directly related to the nature of sediments present. Based on information provided by the Detroit District, Corps of Engineers, St. Marys River sediments range from non-cohesive, gravel-size material to dense clays that are strongly cohesive. These changes may be observed both in the axial direction and transversely at individual river cross sections.

During the period mid-December to mid-January ice begins to accumulate on the St. Marys River. As the season progresses, the ice consolidates into a solid, continuous cover. At any stage in its development, the ice cover may be broken by vessel movement. Commercial vessel activity normally results in a broken channel through an otherwise continuous ice cover. Icebreaking activity may yield a broken ice field across the breadth of the river channel.

MODEL FORMULATION

The numerical model to be presented is based on the premise that in-channel forces resulting from vessel movements are created by backwater velocity, propeller jet velocity and ship-induced waves. It is also assumed that, to a first approximation, the effect of water velocities induced by vessel motion is of a similar nature to the effect of water velocities associated with natural gravity flows. The latter assumption provides the basis for estimating relationships between sediment concentration and flow velocity and for estimating the size and quantities of surficial bottom particles displaced. In this context, flow velocity, as used throughout this report, is the algebraic sum of backwater, propeller jet, and ambient river velocities.

General

As a vessel moves forward in a restricted channel, the water displaced by the movement flows in a direction opposite to vessel motion. Displacement flow velocity increases rapidly as vessel speed approaches the so-called first critical velocity, formulated by Hochstein (1980) as follows

$$V_{cr} = K(gA_c/B_c)^{0.5} \quad (1)$$

where

A_c = the cross-sectional area of the channel (ft)

B_c = the surface width of the channel

g = gravitational acceleration (32.2 ft/s/s)

K = the constrainment factor defined as a function of the blocking ratio $n = A_c/A_m$ and the ratio L/b_m where A_m is the cross-sectional area of the submerged portion of the vessel and L and b_m are vessel length and beam, respectively. The curve which defines K is given by Hochstein (1980). The constant $K \leq 1.0$ in all cases.

As V_{cr} decreases, vessel speeds must also be decreased if adverse effects are to be minimized or prevented. Equation (1) shows that decreasing either K or the ratio A_c/B_c (hydraulic depth) decreases V_{cr}. In both cases, the result is a decrease in the value of the blocking ratio.

Closely associated with displacement flow is the phenomenon referred to as "drawdown." As the result of vessel movement in restricted channels, a displacement wave of depression forms, its phase velocity being equal to the speed of the ship which creates it. At a ship's speed equal to the first critical velocity, the displacement wave becomes a classical "hydraulic jump." The wave can be effective in creating negative impacts in shallow water and at channel banks.

Disturbances also are caused by the propeller jet which may impinge on the channel bed and banks. The jet is in the form of a cone in which the velocity rapidly decreases away from the propeller. Bottom disturbance, thus, is a function of the distance from propeller axis to the bottom. Propeller jet disturbances are greatest at bends in a channel and in reaches where cross-winds may force vessels to move with a substantial angle to the channel axis.

When a ship moves over a water surface, a system of bow waves and a wake are formed. The bow waves and wake are propagated in the form of four trains of diverging and transverse waves formed at the bow and stern, respectively. The midline of the front of the diverging waves makes an angle of about 20 degrees with the vessel trackline. The transverse waves are included inside the diverging wave and their propagation (phase) velocity is equal to ship's speed as is the displacement wave. In shallow water, orbital velocities associated with these surface gravity waves frequently are adequate to resuspend sedimentary material.

Backwat· Velocity

Backwater flow velocity is calculated using an approach developed by Hochstein (1967) which relates the change in flow velocity ΔV_w to vessel speed V_s, blocking ratio and critical velocity, viz.

$$\Delta V_w = V_s[(aB-B+1)^{0.5}-1] \quad (2)$$

and

$$\Delta V_{wmax}/\Delta V_w = \alpha = \max(1, 0.114(B_c/b_m) + 0.715) \quad (3)$$

and is defined as the change in mean streamwise velocity.

In Equation (2), $a = (n/(n-1)^{2.5}$ and $B = 0.3e^{1.8V_s/V_{cr}}$, $V_s/V_{cr} \leq 0.65$ or $B = 1.$, $0.65 < V_s/V_{cr} \leq 1.$ (Hochstein, 1967).

The shape of the flow velocity cross-sectional diagram can be represented by the following function

$$V_w(y) = k_1 e^{(-y/k_2)} \quad (4)$$

where

$V_w(y)$ = the backwater flow velocity (fts^{-1}) at distance y (ft) from the sailing line

$k_1 = V(0) = \Delta V(y)_{max} = \alpha\Delta v$ (i.e., the velocity at the sailing line)

$k_2 = B_1/\alpha\ (1-e^{-\alpha F(\alpha)})$

B_1 = distance (ft) from vessel centerline (sailing line) to shoreline

$F(\alpha) = 0.42 + 0.52 \ln \alpha$

The model yields an evaluation for any point on the channel cross section. In the examples provided in the following section it is assumed that the vessel operates on the channe sailing line and never exceeds the established speed limits.

The relative accuracy of the backwater equation for predicting backwater velocities is shown in Figure 1. The data for Figure 1 were generated during a test of the prediction technique on the Kanawha River in West Virginia. The test was conducted under open-water conditions. Conditions on the Kanawha River where the observations were made (channel configuration, depth, etc.) are not dissimilar from those of the St. Marys River.

Drawdown

Calculations of drawdown heights are based on the approach of Hochstein (1967) which uses Bernoulli's equation as the starting point. With this approach, the total difference in elevation between the undisturbed water surface and the lowest point on the displacement wave is given as

$$\Delta H = V_s^2(a-1)B/2g \qquad (5)$$

The relative accuracy of Equation (5) for predicting drawdown heights is shown in Figure 2. The observations in Figure 2 were extracted from drawdown data collected at seven cross sections along the St. Marys River, and represent 84 usable data points from a total of 94. The data represent open water conditions.

Initial results using Equation (5) shows that drawdown values were consistently underestimated for the Sand Island and West Cell Dock data. Analysis of all cross sections showed, for these two sections, a relatively narrow channel section within a much broader river cross section. A dramatic improvement of the fit of the data from these two sections was achieved by multiplying the calculated ΔH by the term $3.4 - (5.8 \times C_c/B_c)$ where C_c is the width of the maintained channel and $C_c/B_c \leq 0.2$. The data in Figure 2 have been so corrected.

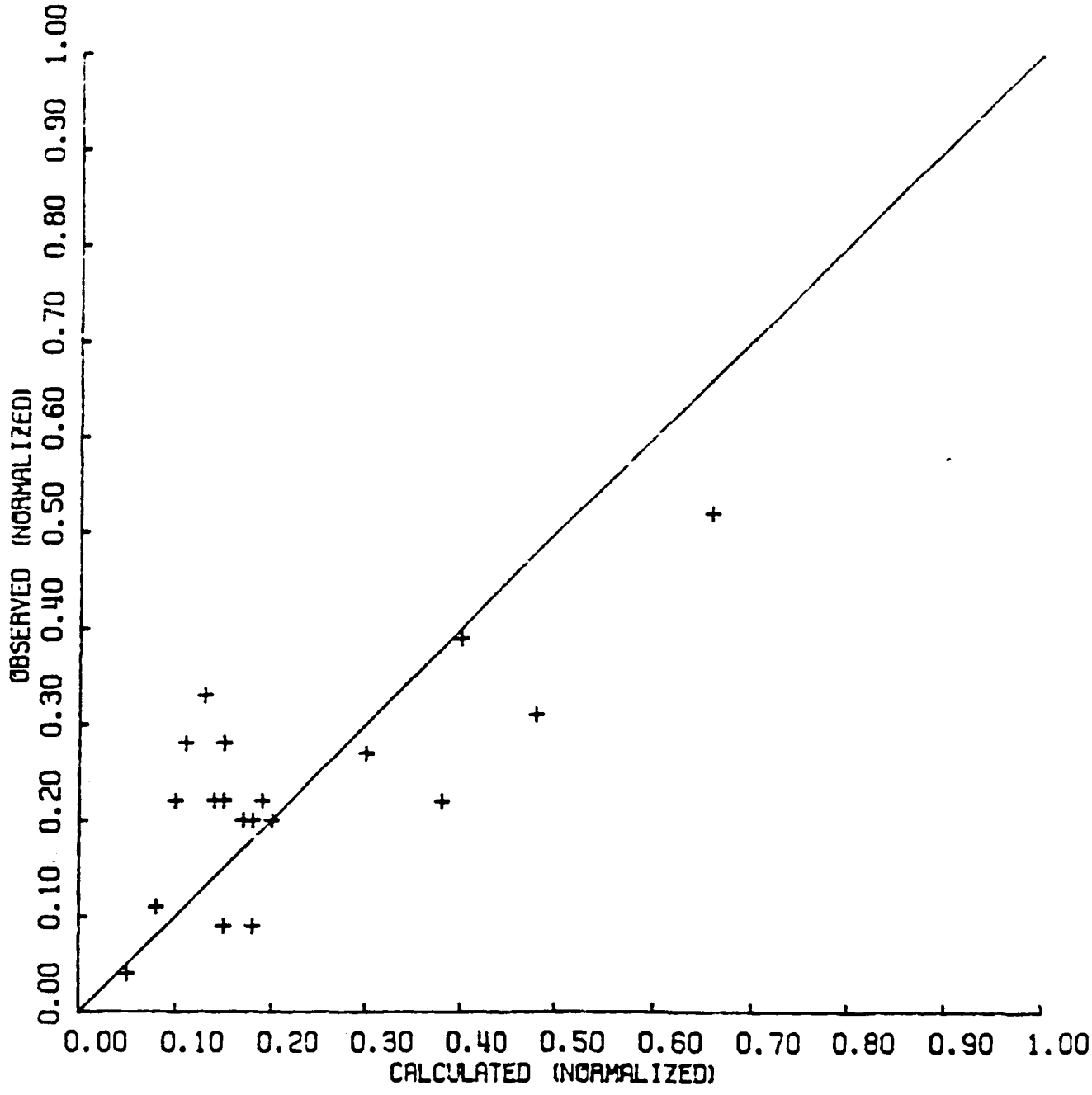

Figure 1.--Correlation plot of measured versus calculated backwater velocities.

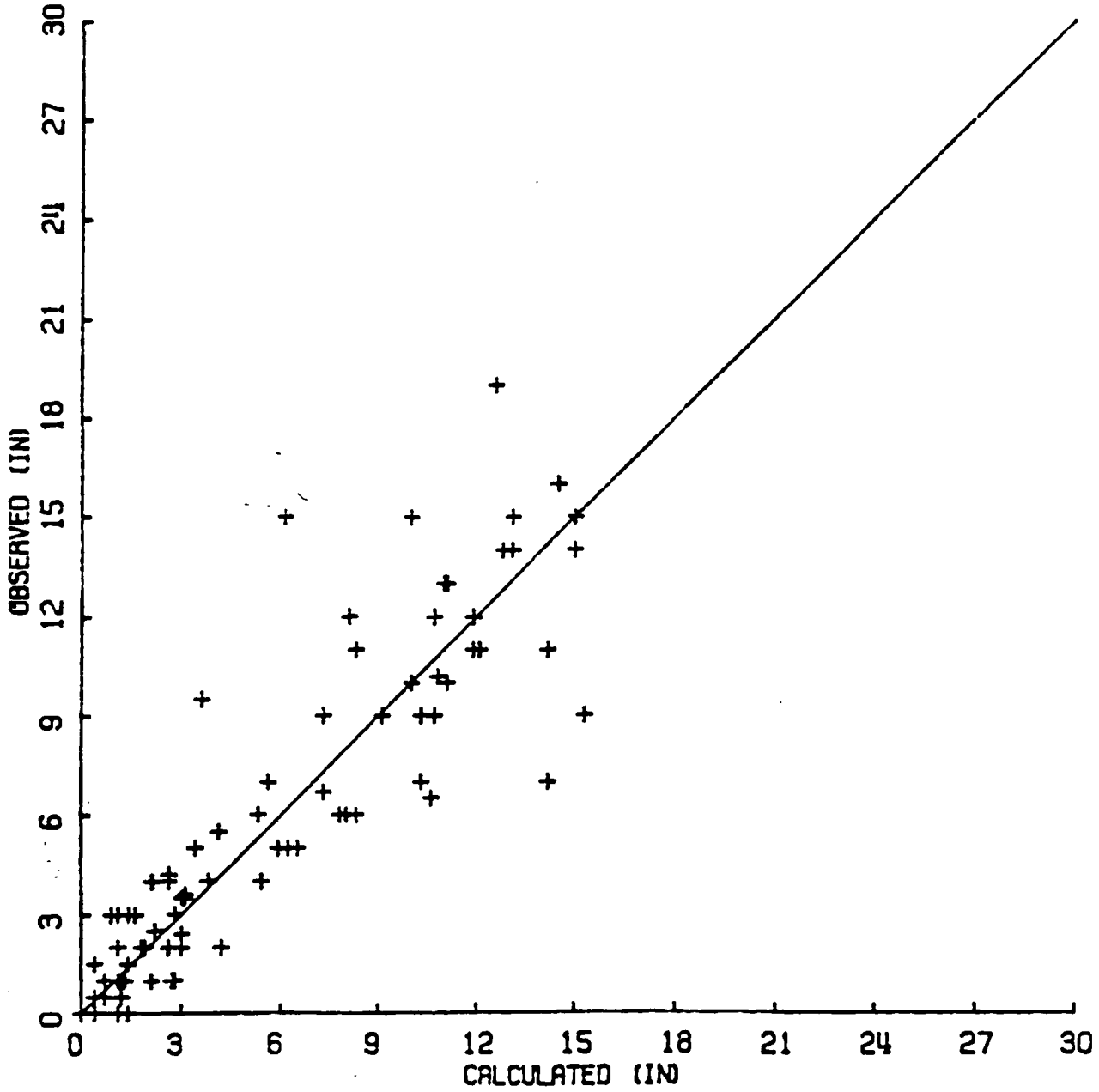

Figure 2.--Correlation plot of observed versus calculated drawdown heights using 84 data points from seven cross sections on the St. Marys River.

Some comments concerning the quality of the observational drawdown data is essential. The level of accuracy at which necessary data was recorded showed some inconsistencies. For example, in some cases vessel draft was recorded to the nearest 0.1 foot or even 0.01 foot, whereas, in others it was only recorded to the nearest whole foot. Tabulated speeds in at least two instances were different than the values that would be obtained by dividing vessel length by the difference in time for bow and stern passage past the recording point. Specifically, the speed of the Edgar B. Speer during a downbound passage on 5/28/85 was given as 9.65 ft/s, whereas, the value calculated using vessel length and time difference was 9.84 ft/s. For the downbound passage of the Canadoc on 5/29/85, tabulated and calculated speed values are 12.54 ft/s and 12.60 ft/s, respectively.

Perhaps the most serious shortcoming of the observational data was the failure to indicate ship position relative to the various observation points. An evaluation of the effect of ship distance on wave height at the channel bank, thus, was impossible. It is assumed here, therefore, that the vessels navigate always on the sailing line. Moreover, no attempt was made during the observation period to separate the effects of drawdown, ship divergent waves and wind-generated surface waves. Calculations here and elsewhere suggest that these complicating factors may be important.

Given the deficiencies in the data, the fit of observations versus calculations shown in Figure 2 is quite remarkable. The goodness of fit is shown statistically as well. The means and standard deviations of the observed and calculated drawdown heights were 6.1, 4.9 and 5.9, 4.7, respectively.

Ice conditions impact on the drawdown effect reflected through reduction in channel cross-sectional area and is manifested by changes in the values of a and B in equation (5).

The relative accuracy of equation (5) to predict drawdown heights under ice based on only seven data points is shown in Figure 3. Although the sample is too small to draw any statistically significant conclusions, for completeness and to provide conservative (calculated values with tendency to be higher than measured) evaluation, the model has been corrected to reflect the difference between observed and calculated drawdown values. The least squares line through the origin shown on Figure 3 has a slope of 1.7 and this is the multiplier of equation (5). Model values for drawdown under ice should be used with caution until additional data becomes available to verify the validity of the correction factor.

Propeller Jet Flow Velocity

Calculations of propeller jet flow velocities are based on the approach of Blaauw and Van de Kaa (1978) which assumes a Gaussian distribution of velocity within the cone of flow behind the propeller.

The maximum propeller jet velocity at a radial distance r from the axis is given as

$$V_{pj}(r) = 1.285\ S\ (D_p\ P_e/S)^{1/3}/r \qquad (6)$$

where

P_e = vessel horsepower

S = the number of propellers

D_p = the propeller diameter (ft)

Figure 4 shows the ability of the method to predict propeller jet velocities. These data were collected at the same time and under similar conditions to those shown in Figure 1.

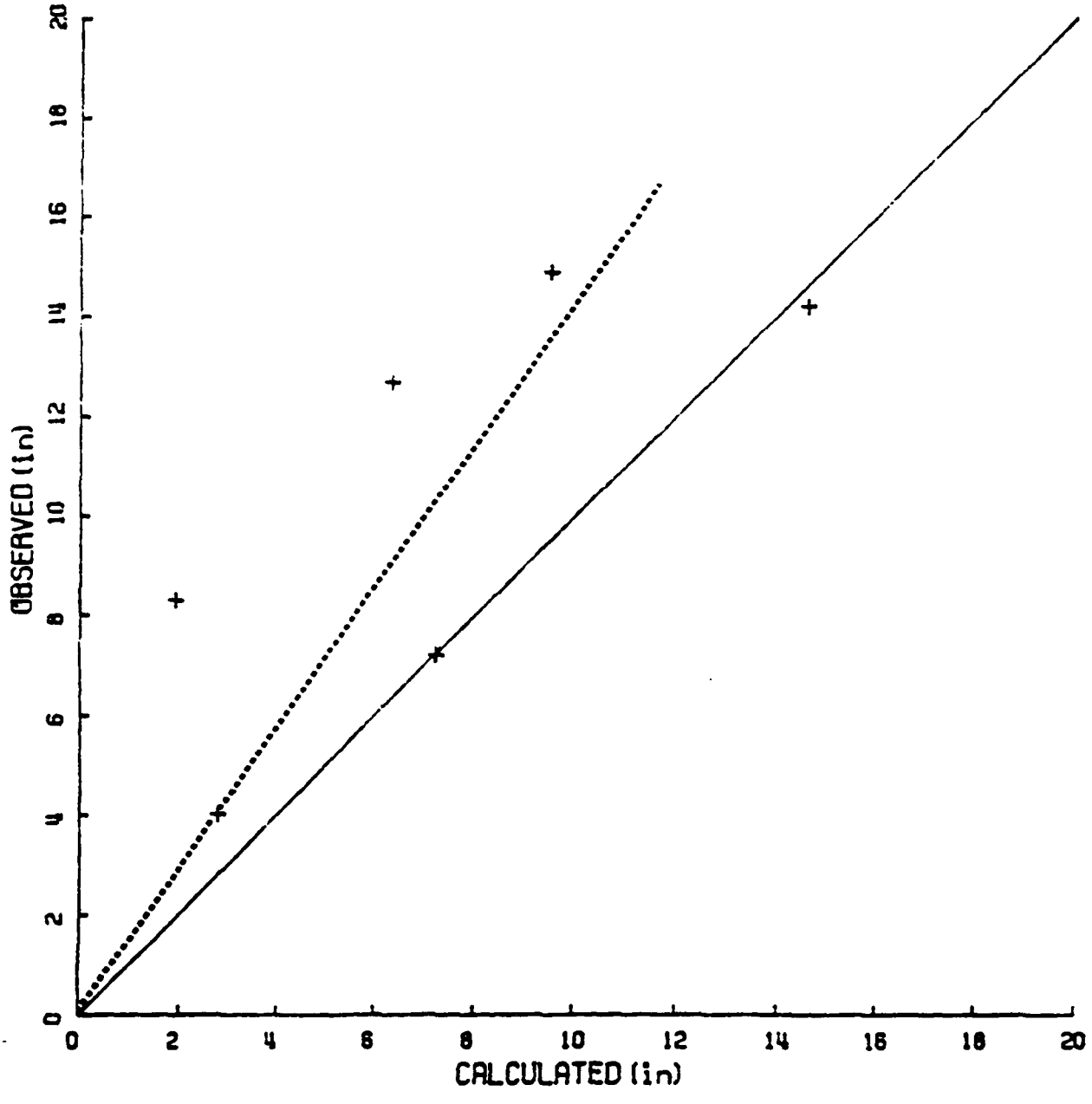

Figure 3.--Correlation plot of observed versus calculated drawdown heights using seven data points (two are identical) from two cross sections on the St. Marys River. Data collected with ice cover present. The broken line is the least squares best fit of the points.

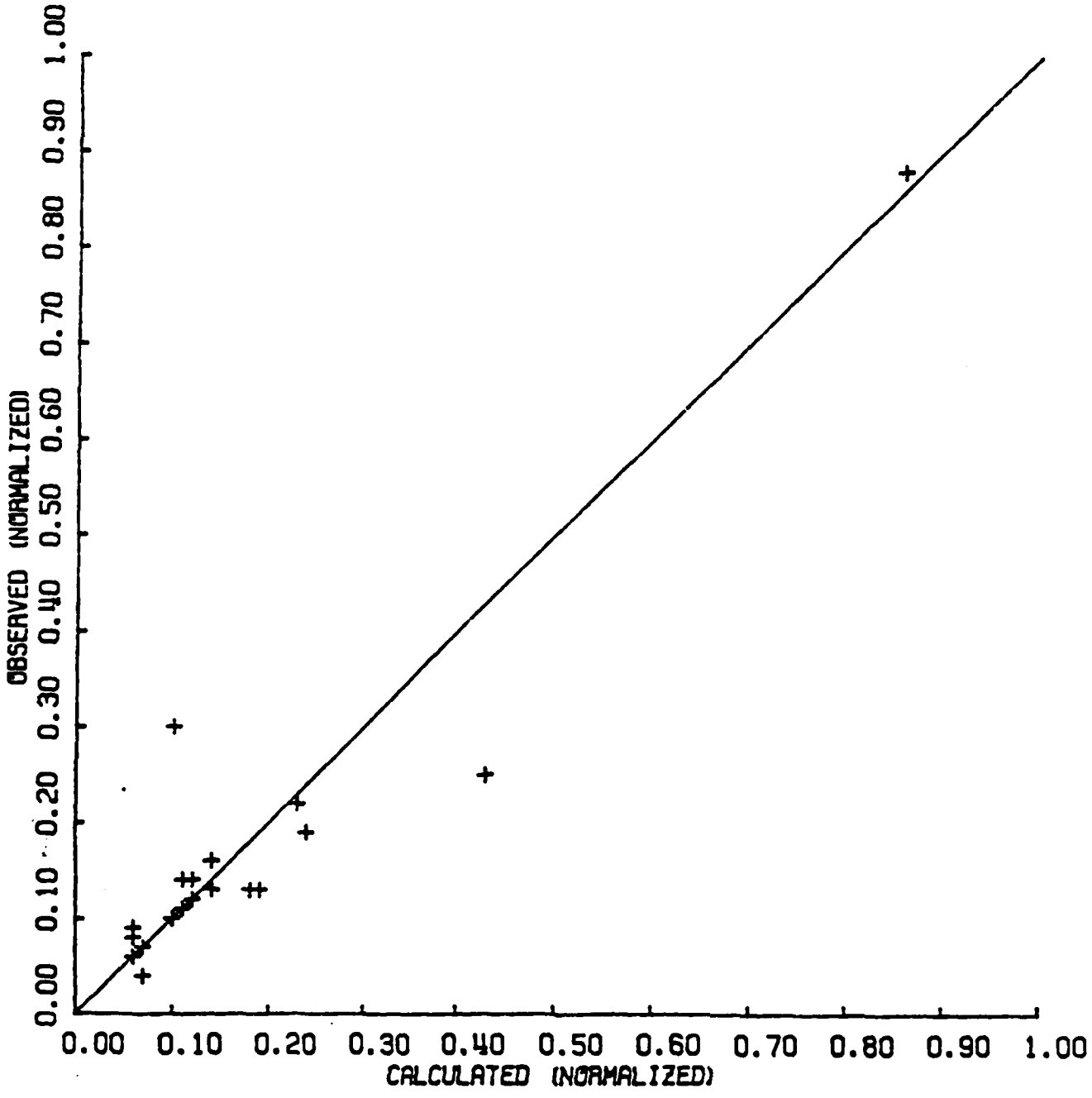

Figure 4.--Correlation plot of measured versus calculated propeller jet velocities.

Ice Operations

Power required for vessel operation at specified speed limits is arrived at with an equation of the form

$$P_e = AV_s^b \tag{7}$$

where

A and b = constants

Using an example given by Wuebben, et.al. (1984) based on a model of the MV ST. CLAIR, the values for the constants in equation (7) were found by a least squares technique to be A = 2.4 and b = 3. The values, of course, are applicable only to open-water operations.

In ice, power required to attain a given speed of advance is substantially greater than is given by equation (7). To accommodate this difference, curves of vessel speed versus ice thickness (Figures 5 and 6) provided by the Detroit District, Corps of Engineers, were used to scale the constants in equation (7). The curves were partitioned into N straight line segments, with N sufficiently large to completely describe the behavior of the curve.

For operations in ice, it was assumed that propeller jet velocity, for the same expenditure of horsepower, increased as the square of the velocity for open-water operations. The factor applied for ice operations thus is (max. vessel speed in open water/vessel speed in ice)^2 and serves to correct both backwater and propeller wash velocities. The maximum propeller jet velocity, of course, is limited by the available vessel power as shown by equation (6). In the example cases to be presented, ice thicknesses prevented vessels from attaining established speed limits even with maximum power expenditure.

Where ice cover is present, channel cross section is effectively reduced. This reduction will result in an increase in K, V_{cr}, V_w, ΔH, and V_{pj} as is shown in Equations 1 through 6.

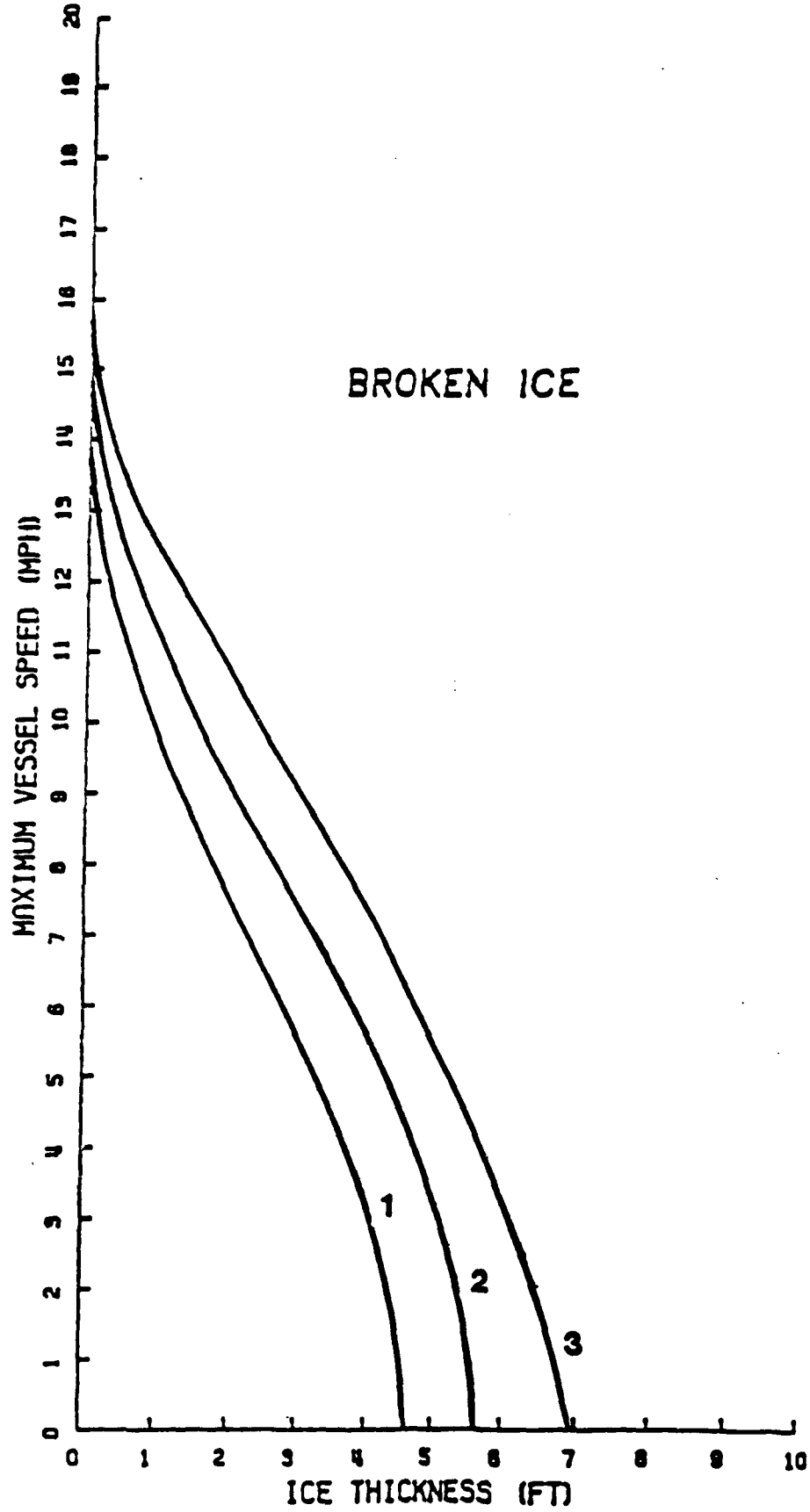

Figure 5.--Maximum vessel speed of advance versus thickness of broken ice.

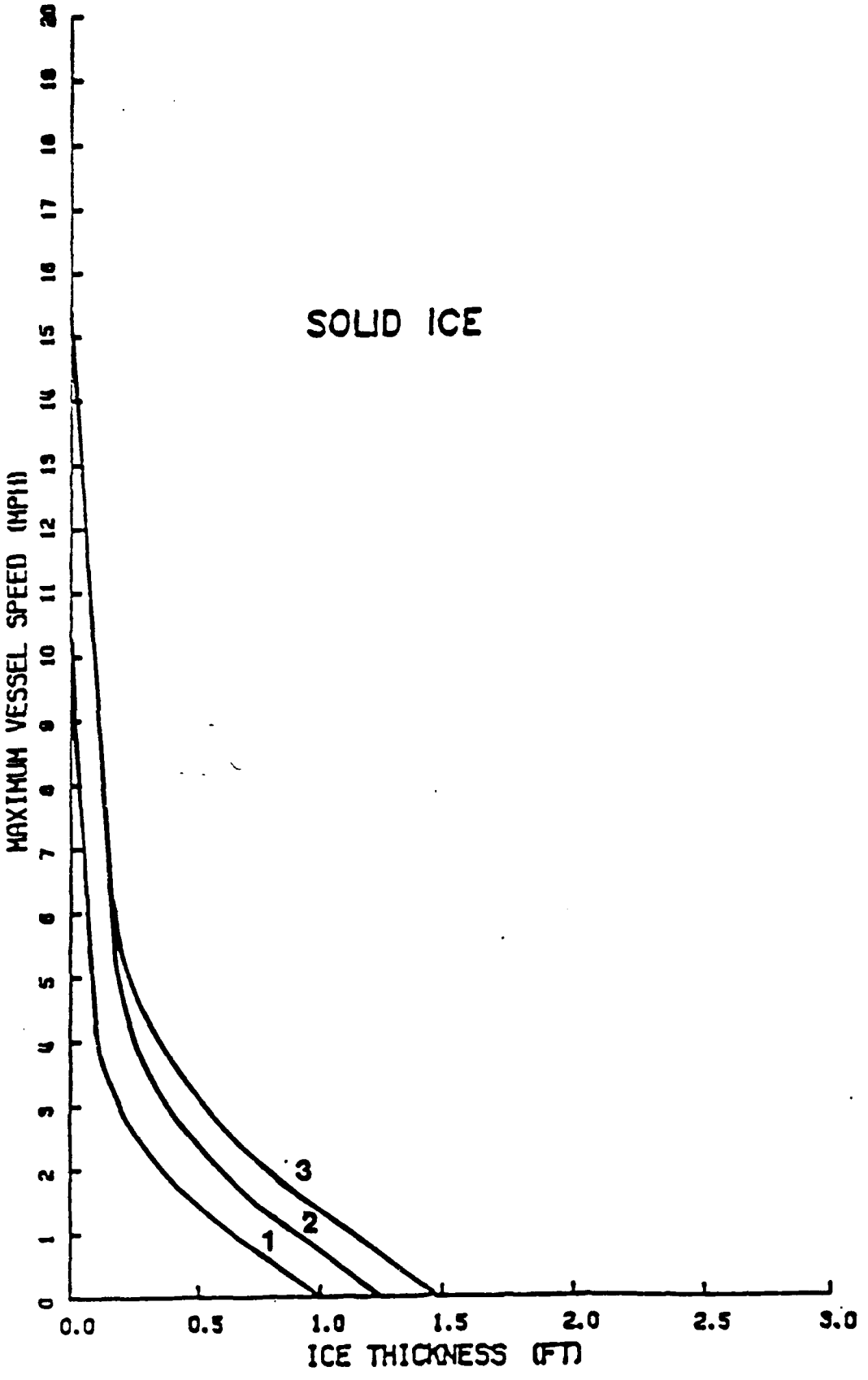

Figure 6.--Maximum vessel speed of advance versus thickness of solid ice.

Under ice conditions, vessel waves are suppressed and additional friction is introduced. Possible impact of these changes is complex and might be accurately described only based on intensive field measurements. In the model, impact of ice-conditions is reflected by empirical coefficient in Equation (5) for drawdown and by reduction in channel cross section.

Surface Waves

For ship operations in channels where the blocking ratio $n > 7$, only diverging waves are important (Hochstein and Adams, 1985). Transverse waves are of minimal impact and can be neglected. Thus, for the St. Marys River with vessel classes 1-10, $n > 15$ always, only diverging waves are treated.

The height of divergent waves as given by Hochstein (1967) is

$$h = 0.0448\, V_s^2 (d_s/L)^{0.5} a \qquad (8)$$

where

d_s = vessel draft.

For most cases of interest, length of divergent waves $l \simeq 10h$ (Hochstein, 1967). A well-known expression which relates maximum bottom wave orbital velocity to wave height, length and period is (e.g. Wiegel, (1964))

$$U_{max} = a\, s/\sinh(k\, D)$$

where

a = wave amplitude

s = radial wave frequency $(2\pi/T)$

k = wave number $(2\pi/l)$

D = water depth

Because wave motions are orbital, wave-associated velocities do not contribute to net channel flow.

Sediment Transport

Two types of soil or sediment disturbance may be expected as the result of ship traffic in restricted channels. The first type, referred to as bed load, occurs when sedimentary particles move in proximity to the bottom. For sediment transport to be classified as bed load, the particles must be in contact with the bottom, at least part of the time. Sedimentary particles carried wholly in suspension and with no bottom contact comprise the suspended load.

Calculations of bed load transport are based on the method of Yalin (1963). The Yalin equation written in terms of the volume flux of sediment per unit flow width is

$$Q = a_1 U_* S\phi[1 - \frac{1}{a_2 S} \ln (1+a_2 S)] \tag{9}$$

where

$a_1 = 0.635$

$a_2 = 2.45 (\rho/\rho_s)^{0.4}[\nu_c/(\rho_s-\rho)g\phi]^{0.5}$

In equation (9), U_* $(=(\nu_o/\rho)^{0.5})$ is the local shear velocity, ν_c is critical shear stress (to be subsequently discussed) ρ and ρ_s are fluid and sediment densities, respectively, and ϕ is the nominal grain diameter. The parameter $S = (\nu_o/\nu_c) - 1$ is the normalized excess shear stress.

Calculations of suspended load transport follow the technique elaborated upon by Smith (1977) and Adams and Weatherly (1981). This method treats a two-phase flow (sediment and water) in which the differential equation of mass conservation represents a balance between upward turbulent diffusion and downward gravitational settling. Integration of this equation for a channel flow situation yields an expresion for sediment concentration, viz.

$$C = \frac{C_o}{1-C_o}\left(\frac{10\phi}{h}\right)^p \exp\left(-\frac{6.24p(z-0.2h)}{h}\right) \tag{10}$$

where

h = water depth

ρ = $w^3/0.4U_*z$ (β = 6.24; Smith 1977)

z = height above bottom

w = particle settling velocity

C_o = a reference concentration

The expression for the reference concentration as developed by Smith and McLean (1977) is

$$C_o = \frac{i\gamma_o C_b S}{1+\gamma_o C_b S} \tag{11}$$

where

i = the fraction of the bed sample in the median size class

$\gamma_o = 2.4 \times 10^{-3}$.

As fluid velocity or bottom stress increases above a sediment bed, a situation is reached such that an additional increase causes sedimentary particles to be put in motion. When motion is incipient, the "threshold" condition has been met. Calculations of sediment threshold are based on the work of Miller, et.al. (1977) for non-cohesive sediments (gravel, sand, coarse silt) and of Migniot (1968) for cohesive materials. These expressions are

$$v_c = 0.32\ Y^{0.5} \qquad \phi < 0.08 \text{ cm} \tag{12}$$

where

Y = shear strength

$$v_c = 46.6\ \phi^{0.54} \qquad 0.08 \text{ cm} < \phi < 0.2 \text{ cm} \tag{13}$$

$$v_c = 79.4\ \phi^{0.9} \qquad \phi > 0.2 \text{ cm} \tag{14}$$

It is important to note that sediments smaller than about 0.02 cm diameter will always move in suspension as was demonstrated by Bagnold (1954) and elaborated upon by McCave (1971).

Model Parameters and Input

Certain, well defined, variables and parameters control the level of fluid velocity induced by propeller jet and backwater effects. The values assigned to each are functions both of vessel (operational parameters) and channel (physical parameters) characteristics. The exact nature of these factors and the manner in which they and their variations are treated in the model have been discussed.

The Great Lakes fleet vessel characteristics required for modeling purposes and the values used in example computations were provided by the Detroit District and are shown in Table 1. It should be noted that operational data for vessel operation in ice, specifically the speed-horsepower relationship could be obtained only for three vessel types, i.e. classes 5, 8, and 10. Values appropriate to classes 6, 7, and 9 were obtained by interpolating the available data. Vessel classes 1-4 were assumed to be unimportant because they are likely to be insufficiently powered, are uncommon, and as a result they are not likely to have much of an environmental effect. Speed-horsepower relationships were available for broken ice navigation as well as for the situation in which a continuous ice cover is present.

The model results focus on two specific examples, Frechette and Ninemile Points (herein after referred to as Sections 1 and 2). The appropriate values of physical and sedimentary characteristics of these areas that are required inputs to the model are shown in Figures 7 and 8 and listed in Tables 2 and 3.

Table 1.--Characteristics of Great Lakes Vessels[1]

(Model Input Values)

Class	Length	Beam	Propellers		Horsepower	Draft (feet)	
	in feet		Number	Diameter (feet)		Upbound	Downbound
1	300	49	1	10.5	3,000	14	20
2	430	60	1	14.0	6,000	20	22
3	524	60	1	14.0	2,500	17	25
4	579	60	1	14.75	4,000	15	26
5	620	68	1	17.5	8,000	18	26
6	680	75	1	18.5	7,000	19	26
7	730	75	1	17.5	9,600	20	26
8	767	75	1	18.5	8,500	19.5	26
9	900	105	1	20.0	13,600	20	26
10	1,000	105	2	17.5	19,500	24	27

[1]Data provided by Detroit District, Corps of Engineers.

Table 2.--Physical characteristics of St. Marys River cross section

Location	Frechette Point (Section 1)	Ninemile Point (Section 2)
Speed limit (ft/s) Upbound	11.7	14.7
Speed limit (ft/s) Downbound	14.7	14.7
Ambient velocity (ft/s)	2.7	0.8
Ice thickness (ft)	0.88	1.11

Table 3.--Characteristics of St. Marys River sediments

Location	Frechette Point (Section 1)		Ninemile Point (Section 2)	
Position	Description	Diameter (mm)	Description	Diameter (mm)
Left bank	Clay	0.004	Clay	0.002
Mid-channel	Clay	0.004	Sand	0.300
Right bank	Clay	0.004	Silt	0.005

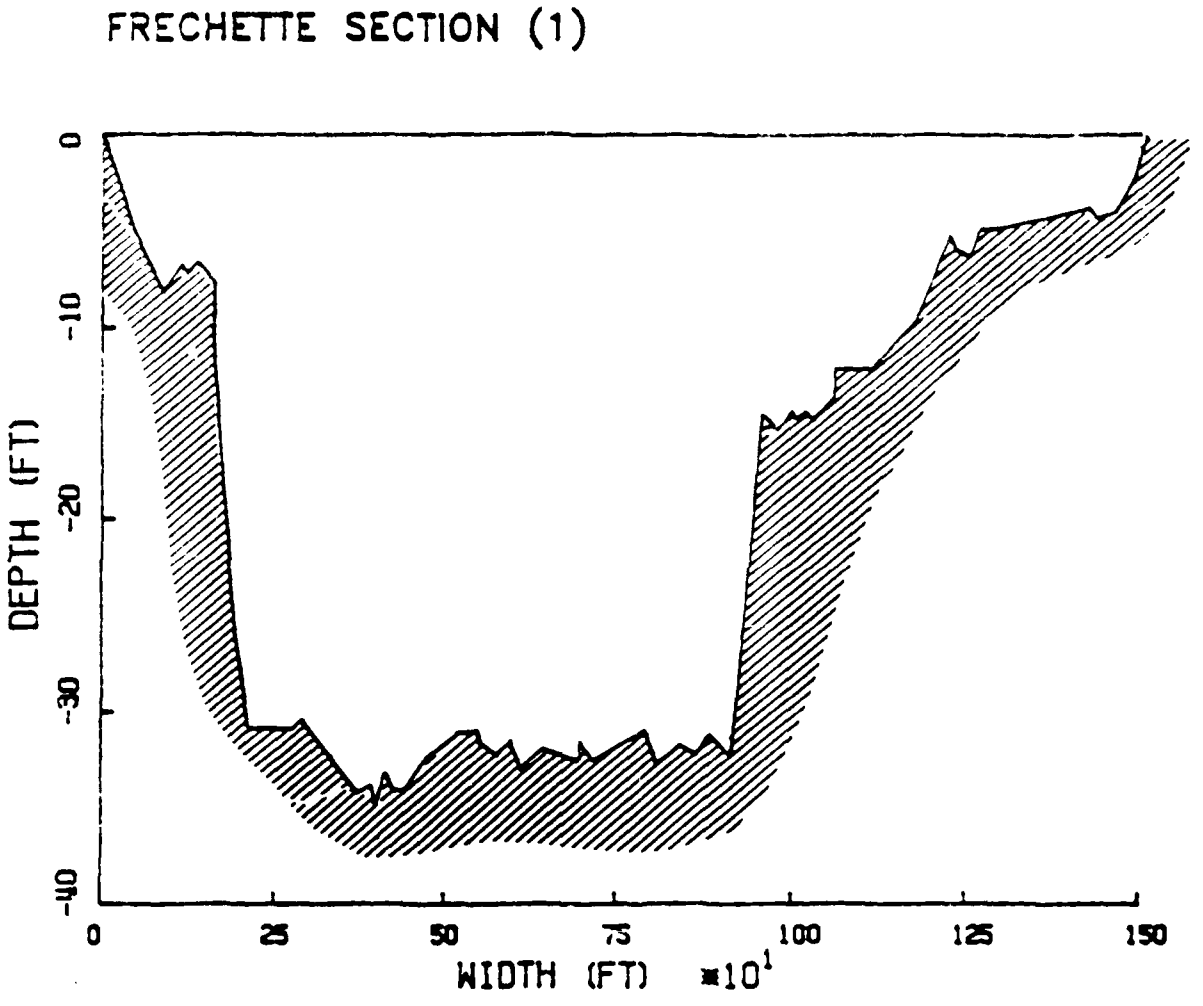

Figure 7.--Frechette cross section (Section 1).

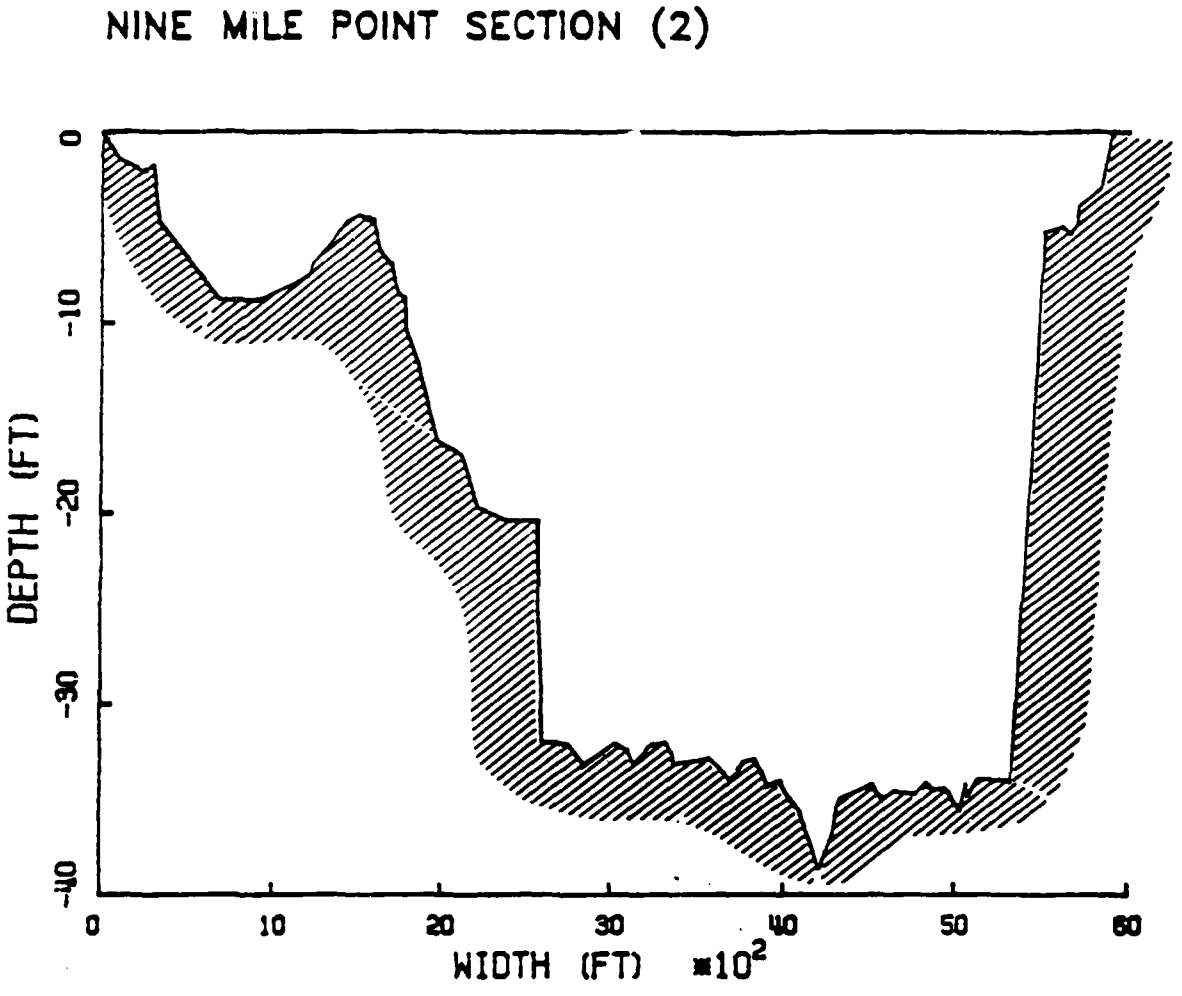

Figure 8.--Ninemile Point cross section (Section 2).

MODEL RESULTS

The results presented below are based on computations using the model described above. Specific outputs of the model include propeller jet, backwater and net velocities, suspended-sediment concentration, bed load sediment flux, kinetic energy density, drawdown and divergent wave height. Kinetic energy density is here defined as one-half times the net-velocity squared. The first six parameters have been calculated at eleven (11) points across a channel section, at the sailing line and at 5 equidistant points either side of the sailing line. Because the navigation channel frequently is nearer one bank than the other, partitioning the cross section in this manner as opposed to equal spacing of points across the entire channel width appropriately weights impacts to that side of the channel on which they are created. Sailing-line values, calculated for upbound and downbound navigation for all 10 vessel classes in open water and 6 vessel classes in ice are shown in Tables 4 and 5 for Sections 1 and 2, respectively. Because of the low power assigned to vessel classes 1-4 (Table 1), it has been assumed that they will be unable to operate in ice. For completeness, however, computations with respect to vessel classes 1-4 have been made and the results are shown in all subsequent data presentations. The model results indicate that vessel impacts with respect to kinetic energy density, suspended-sediment concentration and sediment flux are concentrated at the sailing line. The results to be presented subsequently are for the sailing line unless otherwise indicated. Furthermore, suspended-sediment concentrations represents an average of three values, near-bottom, near-surface, and mid-depth.

Table 4.--Model outputs for Section 1, values given are at sailing line

[E, kinetic energy density; C, suspended-sediment concentration; Q, sediment flux; DD, drawdown]

Ship Type	Ice Free				Broken Ice				Solid Ice			
	E (ft^2/s^2)	C (mg/L)	Q (cm^3/s)	DD (ft)	E (ft^2/s^2)	C (mg/L)	Q (cm^3/s)	DD (ft)	E (ft^2/s^2)	C (mg/L)	Q (cm^3/s)	DD (ft)
1 Upbound---	16	2	0	0.13	---	---	---	---	---	---	---	---
Downbound-	1	0	0	.19	---	---	---	---	---	---	---	---
2 Upbound---	27	5	0	.26	---	---	---	---	---	---	---	---
Downbound-	4	0	0	.30	---	---	---	---	---	---	---	---
3 Upbound---	21	3	0	.20	---	---	---	---	---	---	---	---
Downbound-	7	0	0	.37	---	---	---	---	---	---	---	---
4 Upbound---	18	2	0	.17	---	---	---	---	---	---	---	---
Downbound-	9	<1	0	.39	---	---	---	---	---	---	--	---
5 Upbound---	24	4	0	.27	34	6	0	0.51	19	3	0	0.51
Downbound-	10	<1	0	.47	22	3	0	.90	4	0	0	.90
6 Upbound---	28	5	0	.34	42	8	0	.65	20	3	0	.65
Downbound-	12	1	0	.56	29	5	0	1.05	4	0	0	1.05
7 Upbound---	31	5	0	.37	44	9	0	.70	24	4	0	.70
Downbound-	12	1	0	.56	26	4	0	1.05	6	0	0	1.05
8 Upbound---	29	5	0	.35	41	8	0	.66	23	4	0	.66
Downbound-	12	1	0	.56	24	4	0	1.05	6	0	0	1.05
9 Upbound---	39	7	0	.63	52	10	0	1.21	31	5	0	1.21
Downbound-	20	3	0	.98	35	7	0	1.89	11	1	0	1.89
10 Upbound---	72	15	0	.86	113	25	0	1.65	98	22	0	1.65
Downbound-	38	7	0	1.05	78	17	0	2.02	65	14	0	2.02

Table 5.--Model outputs for Section 2, values given are at sailing line

[E, kinetic energy density; C, suspended-sediment concentration; Q, sediment flux; DD, drawdown]

Ship Type	Ice Free				Broken Ice				Solid Ice			
	E (ft^2/s^2)	C (mg/L)	Q (cm^3/s)	DD (ft)	E (ft^2/s^2)	C (mg/L)	Q (cm^3/s)	DD (ft)	E (ft^2/s^2)	C (mg/L)	Q (cm^3/s)	DD (ft)
1 Upbound---	8	0	0	0.06	---	---	---	---	---	---	---	---
Downbound-	7	0	0	.08	---	---	---	---	---	---	---	---
2 Upbound---	14	0	0	.10	---	---	---	---	---	---	---	---
Downbound-	9	0	0	.11	---	---	---	---	---	---	---	---
3 Upbound---	11	0	0	.08	---	---	---	---	---	---	---	---
Downbound-	13	0	0	.12	---	---	---	---	---	---	---	---
4 Upbound---	9	0	0	.07	---	---	---	---	---	---	---	---
Downbound-	15	0	0	.13	---	---	---	---	---	---	---	---
5 Upbound---	12	0	0	.10	14	0	0	0.19	8	0	0	0.19
Downbound-	15	0	0	.15	19	0	0	.26	8	0	0	.26
6 Upbound---	13	0	0	.12	16	0	0	.20	8	0	0	.20
Downbound-	14	0	0	.16	20	0	0	.31	8	0	0	.31
7 Upbound---	14	0	0	.12	20	0	0	.22	10	0	0	.22
Downbound-	14	0	0	.16	25	0	0	.31	10	0	0	.31
8 Upbound---	14	0	0	.12	20	0	0	.22	9	0	0	.22
Downbound-	14	0	0	.16	24	0	0	.31	9	0	0	.31
9 Upbound---	15	0	0	.18	23	0	0	.34	13	0	0	.34
Downbound-	17	0	0	.26	29	0	0	.49	13	0	0	.49
10 Upbound---	34	0	0	.23	71	<1	<1	.44	54	0	0	.44
Downbound-	34	0	0	.28	82	<1	<1	.53	60	0	0	.53

It is important to note that the accuracy of model output values are strongly dependent on the quality of input parameters, particularly in the case of turbidity and suspended sediments. These outputs must, therefore, be viewed in the context of parametric inputs.

Shown in Figure 9 is the kinetic energy density associated with each vessel class for open-water and ice navigation through Section 1. In this and subsequent portrayals, ICE 1 refers to broken ice while ICE 2 represents a solid ice sheet. The values shown are for the sailing line. Kinetic energy density decays to not more than 6 percent of the sailing line value at the first grid point on either side of the sailing line. Thus, almost 95 percent of the kinetic energy associated with ship passage is confined to the center of the channel.

Several interesting aspects of the problem emerge from Figure 9. In each case, i.e. open water, ICE 1 or ICE 2, the kinetic energy per vessel passage is greater for an upbound (empty) transit than for a downbound (loaded) one. Also, kinetic energy densities associated with navigation of vessel classes 5-10 in ICE 1 (broken) are greater than those associated with operations in ICE 2 (sheet) ice. Finally and perhaps most significantly, the magnitude of the energy effects of vessel class 10 is substantially greater than the other nine classes. For example, kinetic energy associated with an open water, upbound passage of a class 10 vessel is greater than that for any other vessel operating in ice, regardless of the direction of travel. The magnitude of kinetic energy effects of a class 10 vessel are, in the worst case, about twice as great as those of any other vessel class. The greater forces generated by vessel class 10 are apparently explained by at least three reasons: (1) the only vessel type with 2 propellers, (2) high horsepower and ability to maintain high speed in ice conditions, and (3) a draft of 27 ft.

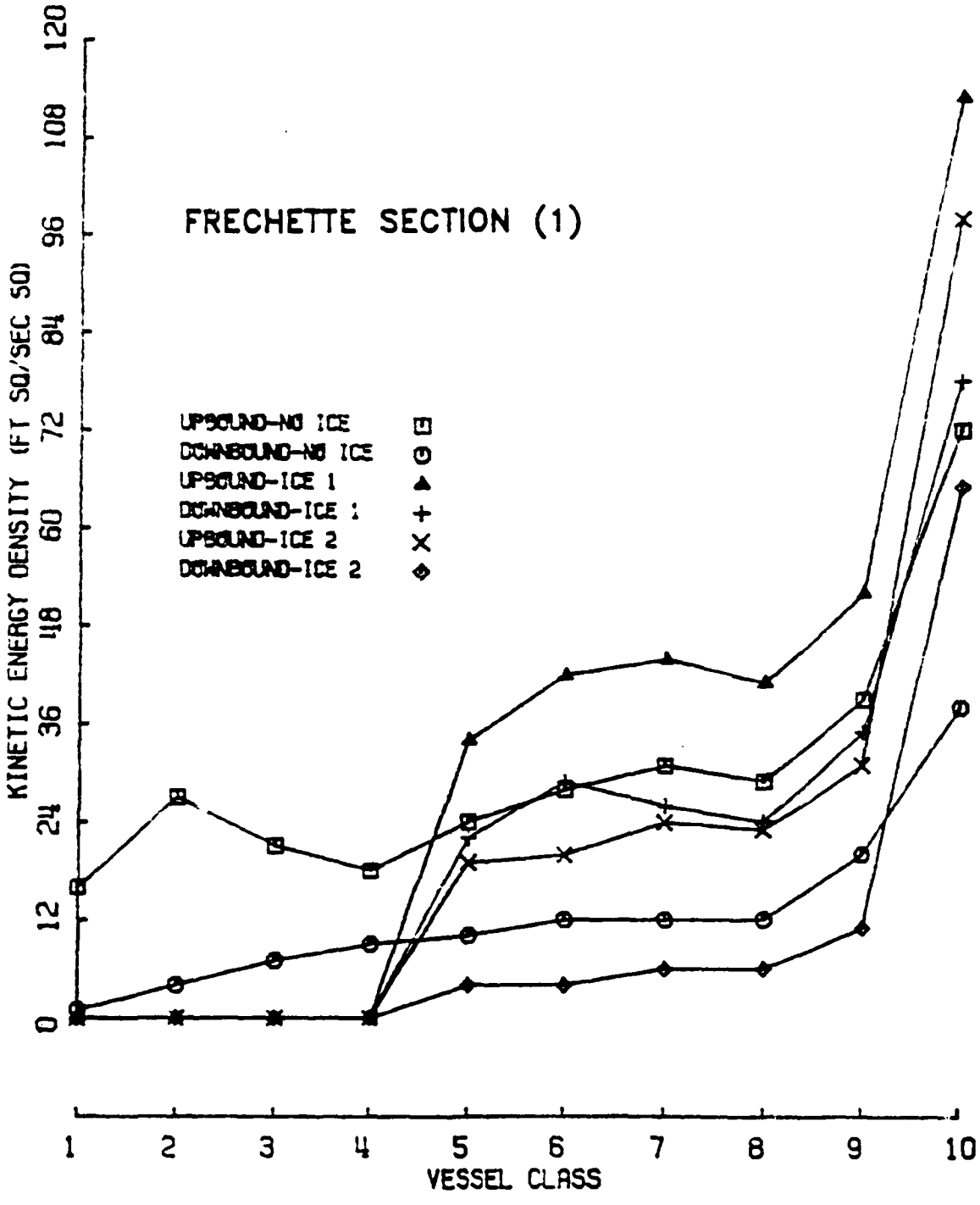

Figure 9.--Curves of kinetic energy density versus vessel type, Section 1, at the sailing line.

Examination of Figure 10 which is kinetic energy density at the sailing line associated with navigation through Section 2 yields results somewhat different from those found for Section 1. For example, the magnitudes of kinetic energy are lower for most vessel classes. This can be directly related to the greater cross-sectional area of Section 2. For vessel classes 1, 2, 7, 8, and 10, in open water kinetic energy per vessel passage is greatest for an upbound vessel, whereas, for vessel classes 3-6, and 9, it is greatest for a downbound vessel. For a class 10 vessel, kinetic energy effects for upbound and downbound vessels in open water are the same. In ice, kinetic energy per vessel passage for all classes is greater for a downbound transit. While the absolute magnitudes at Section 2 are smaller than at Section 1 the relative effect of a class 10 vessel is somewhat greater at Section 2 (i.e. the worst case situation at Section 2 yields a ratio of approximately 3).

As noted above, at Section 1, kinetic energy per vessel passage is always greater for an upbound then for a downbound vessel. At Section 2, however, certain vessel classes induce a greater affect when downbound in open water; downbound passages in ice induce a greater affect than upbound passages for all vessel classes. The reason for these differences is due to the difference in cross-sectional areas of the two sections and the associated ambient velocities. For upbound vessels, propeller wash, backwater, and ambient velocities have the same sign, whereas, for downbound vessels, propeller wash,

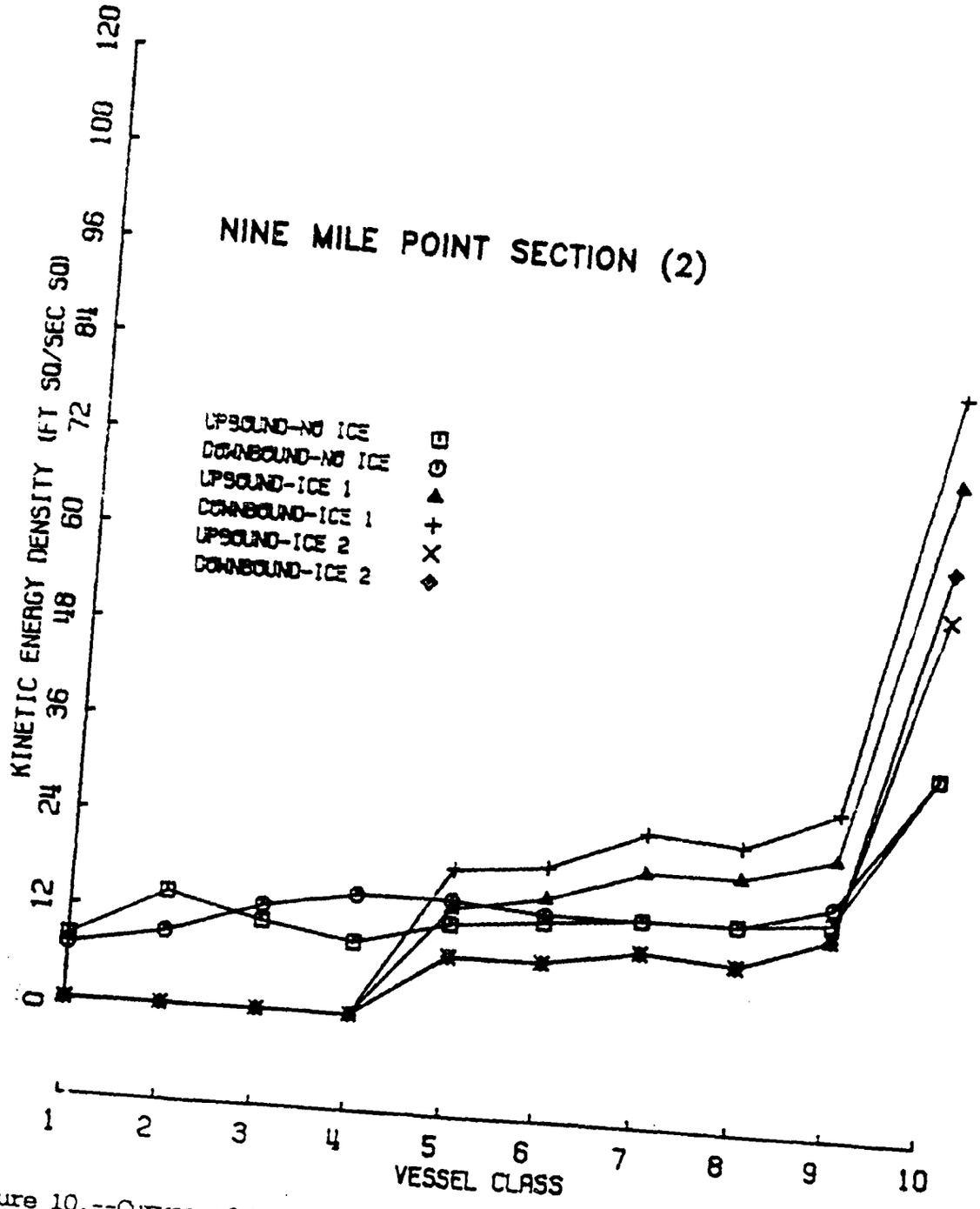

Figure 10.--Curves of kinetic energy density versus vessel type, Section 2, at the sailing line.

and backwater velocities are of opposite sign to that of ambient velocity. Backwater and propeller wash velocity are greater for downbound vessels as the blocking ratio is smaller and the propeller axis is nearer the channel bed because of the greater draft. Thus, at Section 1, the effects of upbound passages of class 5 vessels will always be greater than downbound passages as long as ambient velocity is greater than 1.5 ft/s. At Section 2, because ambient velocity is less than 1.0 ft/s, a downbound passage of a class 5 vessel will induce a greater affect than an upbound passage. Similar reasoning applies to the other vessel classes as well.

The absolute impact of downbound (loaded) vessels is, however, always higher due to associated smaller blocking ratio and similar vessel speeds. This is manifested in higher drawdown values for downbound vessels.

Suspended-sediment concentrations induced at the sailing line at Section 1 by the passage of the various vessel classes are shown in Figure 11. The relationships between suspended-sediment concentration and vessel class are similar to those between kinetic energy density and vessel class shown in Figure 10. Suspended-sediment concentrations induced by the passage in open water of vessel classes 1-9 range from 0-7 mg/L. When ice is present these values may increase slightly. A maximum of 10 mg/L can be associated with vessel class 9 in broken ice. The effect of vessel class 10 is to create a suspended-sediment concentration 2-3 times greater than that resuspended by other vessel types. The difference in sediment concentration between open-water and ice navigation for class 10 is approximately 20 mg/L.

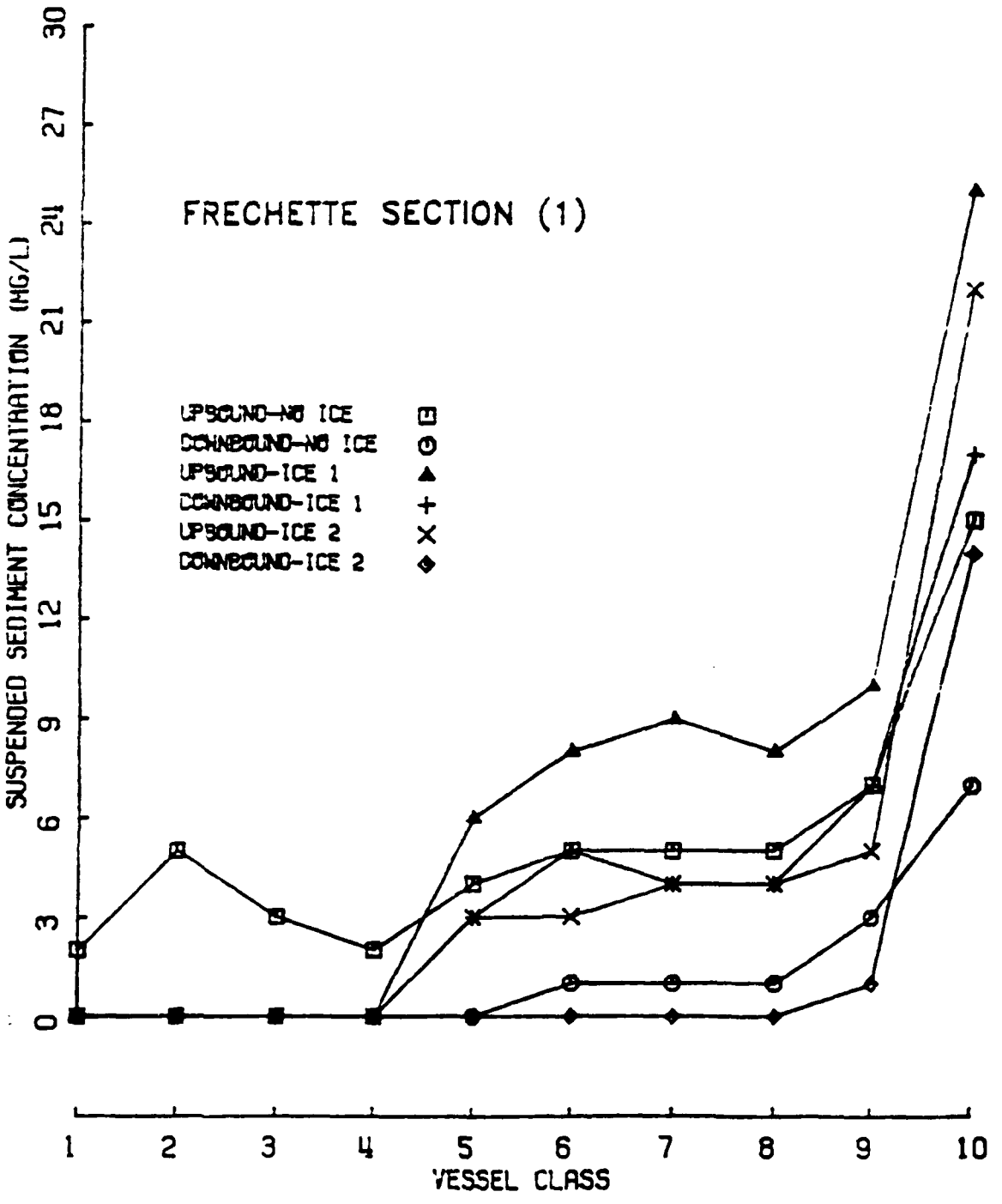

Figure 11.--Curves of suspended-sediment concentration versus vessel type, Section 1, at the sailing line.

At section 2, the bottom remains undisturbed for all vessel classes in open water and in sheet ice. Passage of a class 10 vessel through broken ice resuspends only trace quantities of sediment (Table 5). The difference in sediment resuspension at Sections 1 and 2 is due not only to the difference in cross-sectional areas but also to the prevalence of cohesive sediments at Section 1. It should be recalled that the suspended-sediment concentrations shown in Figure 11 are depth weighted averages of three values (near bottom, near surface, and mid-depth).

Passages of class 1-10 vessels through Section 1 failed to create any bed load transport. This result is expected because of the absence of particles of a size that would normally move as bed load. Although the presence of sand at Section 2 makes bed load transport possible the model predicts only trace amounts of sediment flux induced by class 10 vessels operating in broken ice (Table 5). For upbound transits, sediment would be displaced in a downstream direction. For downbound transits sediment moves upstream.

Drawdown heights, as calculated at the bank, are shown in Figures 12 and 13 for Sections 1 and 2, respectively. The curves in both figures are similar in that vessel classes 5-8 create drawdown waves of similar height, the waves created during ice operations being about 90 percent higher than those generated during open water passages. The magnitude of drawdown in broken and solid ice is about the same. The maximum height of the drawdown waves for vessel classes 5-8 is about 0.6 foot in Section 1 but only about 0.3 foot in Section 2. Drawdown elevations are about twice as large for vessel classes 9 and 10 than they are for the others. Here again the values associated with ice passages are about 90 percent greater than those for open water operations.

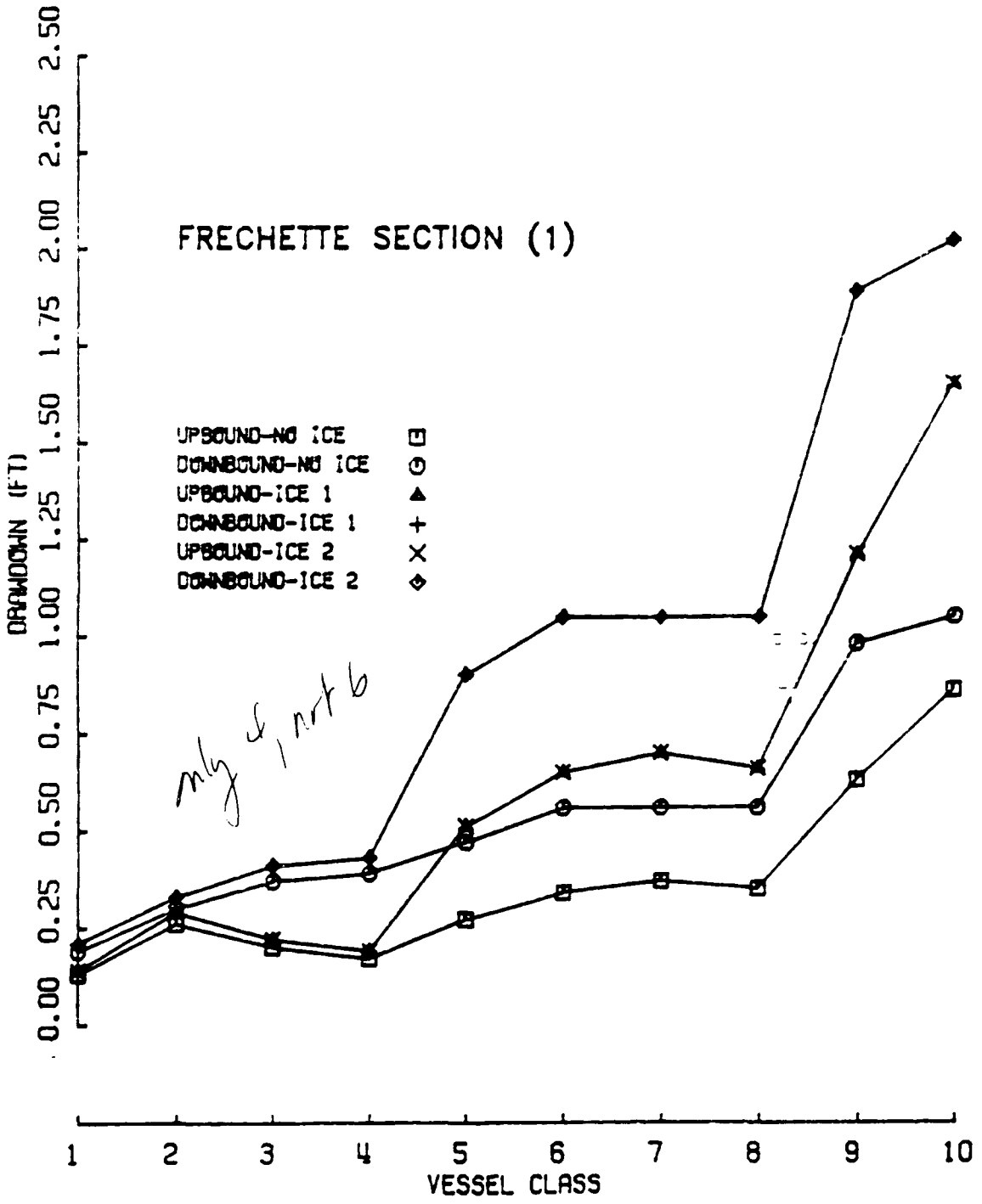

Figure 12.--Curves of drawdown versus vessel type, Section 1.

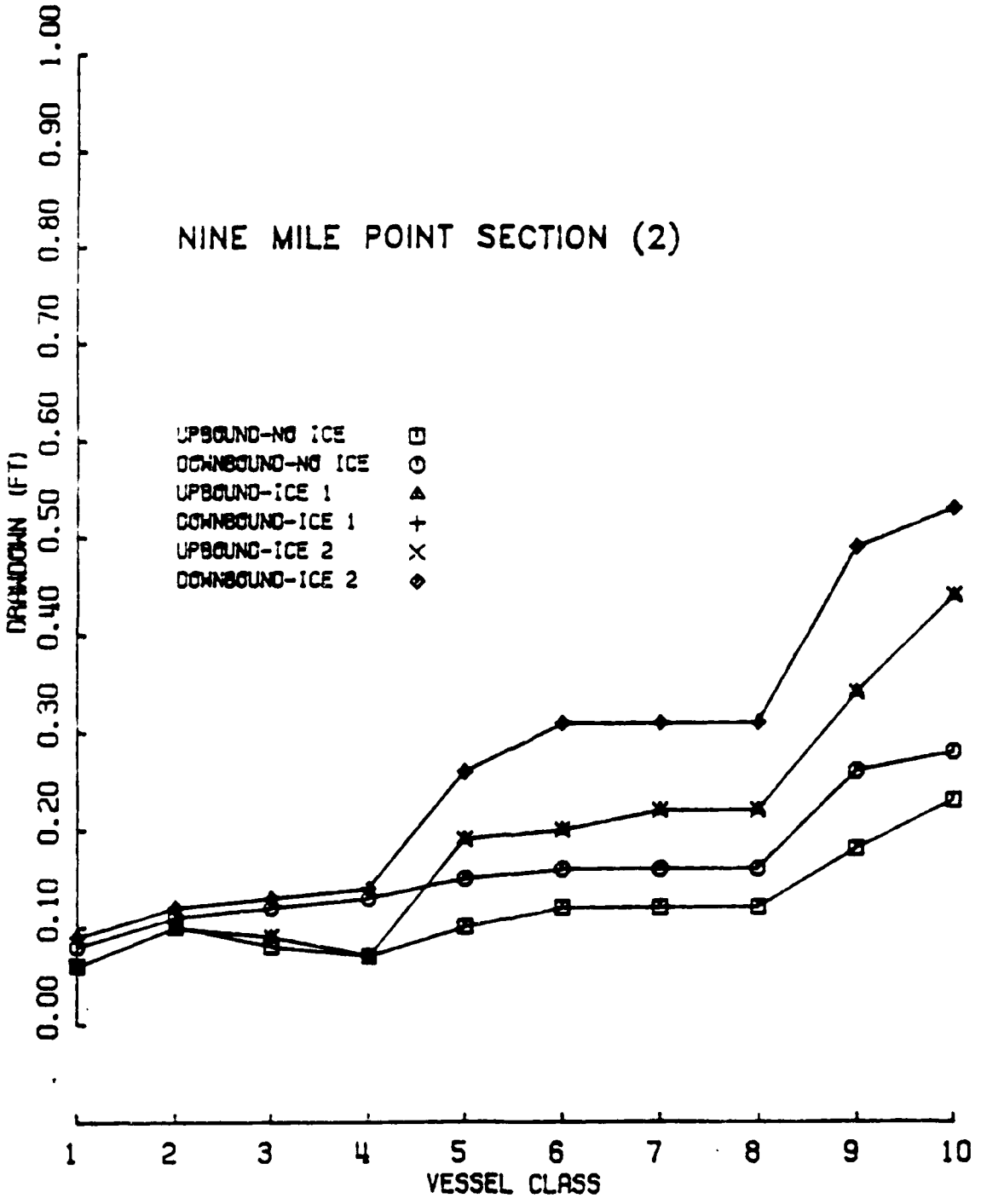

Figure 13.--Curves of drawdown versus vessel type, Section 2.

A significant difference between this model and an earlier version is the incorporation of the effects of diverging waves in the current one. A result of this additional feature is the ability to estimate resuspension of sediments at the banks by orbital motions. Model results show that divergent waves do indeed resuspend sediments in the shallower parts of the cross section. In the cases tested here, resuspended materials were never more than 2 mg/L and frequently were substantially less. It is difficult, however, to isolate the effects of divergent waves from those of drawdown. It is possible that many of the impacts attributed to drawdown may be due to divergent waves or perhaps to a combination of the two.

To summarize the effects of vessel passages on the resuspension of channel sediments it is sufficient to consider vessel classes 5 and 10 only at Section 1. Shown in Table 6 are the relative increases of suspended sediment for class 5 and 10 vessels as a result of the presence of the two different ice types. The downbound, ice free condition is taken as unity.

Examination of the data of Table 6 yields some interesting results with regard to the different influences of the two different ship types on the cross section studied. Perhaps the most significant point is that the range of relative increase of suspended sediments for the three variables considered, i.e. vessel type, vessel direction, and ice type is substantially different, varying from 0 to 25, the latter value associated with an upbound class 10 vessel in broken ice. The smallest impact of a class 10 vessel is similar to the largest impact of a class 5 vessel. In general, due to the small increase in water velocity generated by a vessel relative to ambient water velocity, upbound values are higher than downbound values.

Table 6.--Relative abundances of suspended sediment

Ship Type	Section 1		
	Ice Free	Broken Ice	Solid Ice
5 Upbound---	4	6	3
Downbound-	1	3	0
10 Upbound---	15	25	22
Downbound-	7	17	14

To examine the cumulative effects of vessel traffic for an entire year, the sum of the product of vessel kinetic energy density times the number of vessel transits (Table 7) was calculated. The data are plotted in Figures 14 and 15 with curves for the season ending December 15, for an extension of the season to January 1, and for an extension of the season to February 15. The curves merge and are essentially indistinguishable. The result of the season extension, thus, is a negligible increase of total energy density at Sections 1 and 2. It should be noted that the period of December 15-February 15 was assumed to be characterized by a broken rather than a solid ice cover. Higher impacts are associated with the broken cover than with the solid cover.

Table 7.--Vessel Traffic Scenario Extended Season Navigation

	Passages through the Sault Locks		
	U.S.	Prejected Canadian	Total
1 Apr - 15 Dec 1979	6,452	3,814	10,266
Vessel class breakdown			
ten	2,586	1	2,586
eight	1,374	1	1,375
seven	808	2,287	3,095
six	485	286	771
five	2,101	572	2,673
four	215	15	230
three	162	-----	162
two	107	126	233
one	242	286	528
Direction to 15 Dec			
upbound	4,121	1,767	5,888
downbound	3,959	1,807	5,766
16 Dec - 1 Jan 1980	100	43	143
Vessel class breakdown			
ten	12	-----	12
nine	4	-----	4
eight	18	1	19
seven	7	2	9
six	10	1	11
five	47	2	49
* two	22	22	
* one	2	15	17
2 Jan - 15 Feb 1980	64	28	92
Vessel class breakdown			
ten	8	-----	8
nine	2	-----	2
eight	19	-----	19
seven	4	1	5
six	7	-----	7
five	24	2	26
* two	-----	14	14
* one	-----	11	11
Direction after 15 Dec			
upbound	7	27	34
downbound	157	44	201

Vessel classes one and two are included in class five.

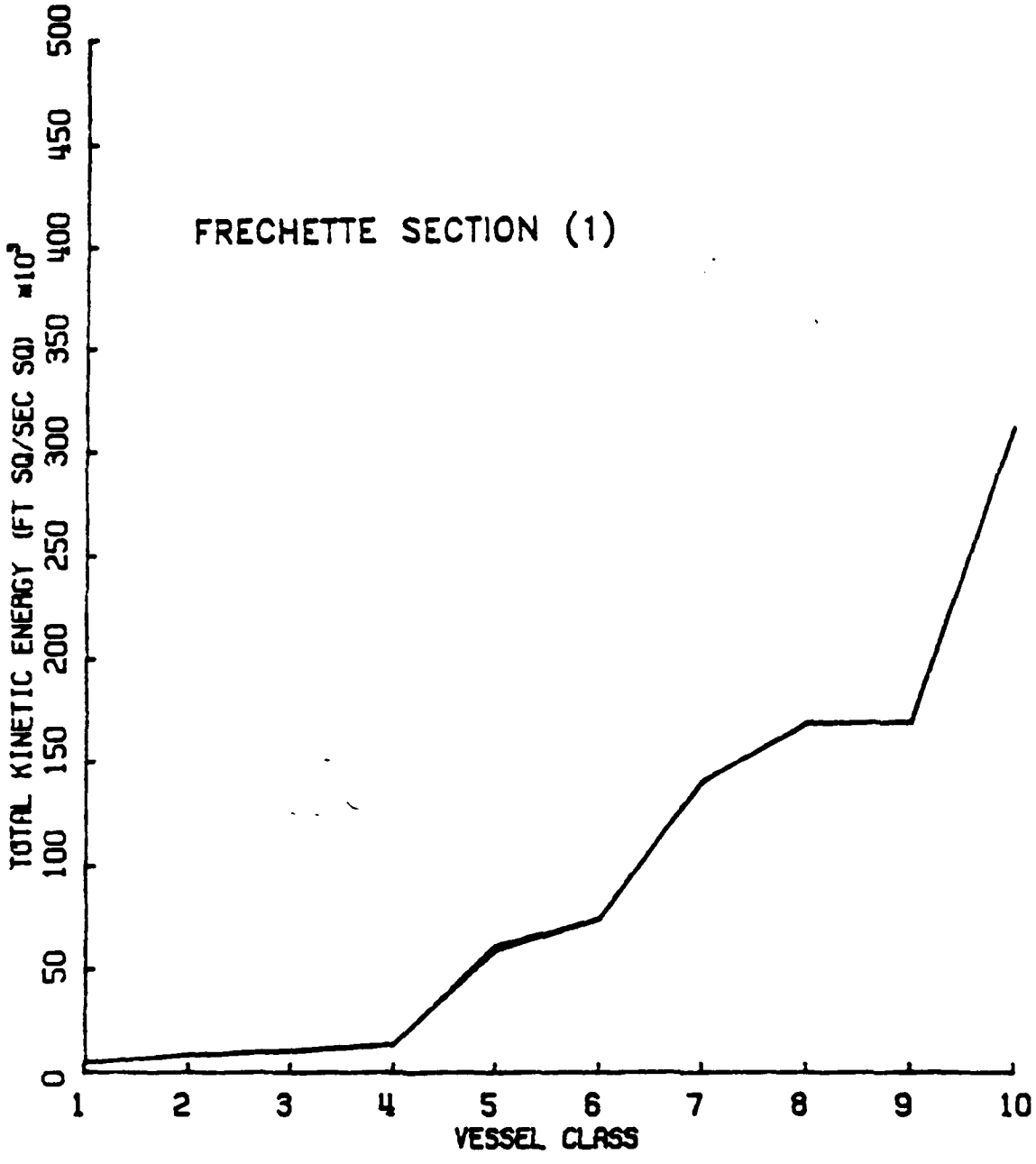

Figure 14.--Total kinetic energy density versus vessel type for a normal season (lower curve) for an extension to January 1 (middle curve), and for an extension to February 15, Section 1.

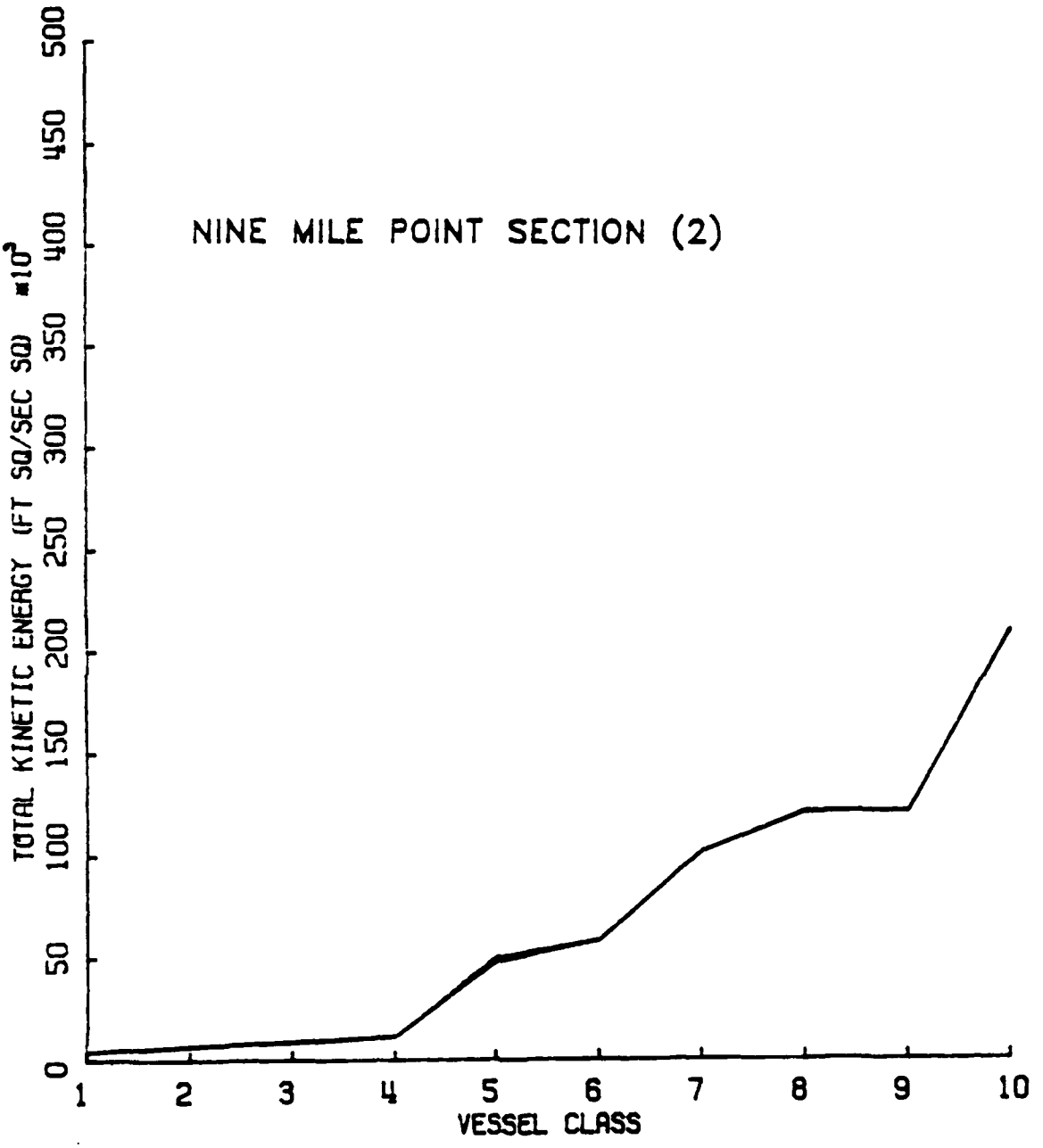

Figure 15.--Total kinetic energy density versus vessel type for a normal season (lower curve) for an extension to January 1 (upper curve), and for an extension to February 15, Section 2.

Finally, it is of practical interest to consider the duration over which a sediment resuspension event initiated by a vessel passage has a detectable impact upon suspended-sediment concentration at a given cross section. Hochstein and Adams (1985) present a method for estimating duration of impact of resuspension that incorporates vessel motion and particle settling velocity. The appropriate expression is

$$DI = L/(V_s \pm V_a) + D(d) \qquad (15)$$

where

DI = impact duration

V_a = ambient river velocity

D = duration of particle settling

d = particle diameter

and the other terms are as given previously. The particle settling velocity, of course, is difficult to define in a heterogeneous size assemblage of particles. When the size distribution is poorly known this problem becomes more difficult and it is, perhaps, better to frame the problem in terms of maxima and minima.

In the case of Section 1, data provided by the Detroit District, Corps of Engineers, indicates the bottom near mid-channel to be composed of firm clay. Clay particle "diameters" generally range from about 1 to 4 microns. Information provided by Hodek, et.al. (1985, p. AA7) indicates that sediments from near mid-channel may be as coarse as 75 microns. Settling velocity w, of these particle sizes in water of 18°C is 1.36×10^{-3} cm/s for 4 micron particles and 4.41×10^{-1} cm/s for 75 micron particles (Gibbs, et.al., 1971). For these values of w, the second term in equation (15) above, thus, ranges from about 100 hours to only 18 minutes where water depth is taken as 16 ft (one-half the depth at Section 1). The first term is much less than the second and for the purpose of estimating impact duration, it may be neglected.

For very fine particles with low settling velocities, the potential for significant increases of suspended-sediment concentration is great. The absence of a noticeable degradation of water quality during the open water navigation season suggests that if sediments indeed are eroded by the passage of ships through Section 1, those sediments must be substantially coarser than 4 microns. Calculations based on data from Table 7, indicate that there is a ship passage about every 34 minutes during the open water navigation season. With an impact duration of only 18 minutes, all material resuspended by one vessel has settled to the bottom before another vessel passes. For extensions beyond December 15, the difference between impact duration and vessel passage period is even greater.

There are, of course, no impacts at Section 2 as materials are neither resuspended or moved as bed load.

MODEL CALIBRATION

The model detailed above has been calibrated with the best information available. Selection of parameter values was made by an analysis of data available from the St. Marys River and other similar aquatic environments, most notably the Kanawha River in West Virginia.

The basic equations in the model have shown good fit with empirical data. Wherever necessary, some of the equations have been modified or new empirical coefficients introduced, to reflect specifics of the St. Marys River hydrographic features. As the result, the presented model provides credible accuracy and sufficiently describes magnitude and tendencies of the very complex effects generated by a vessel movement in a restricted channel. The model provides functional relationships between a variety of variables, determining extent of physical impacts of commercial navigation during both normal and extended navigation seasons. Calibration has shown that the model

results by level of accuracy and scope, as they relate to the magnitude of the effects, are sufficient to make reliable conclusions regarding extent of impacts due to different options of commercial navigation in the Great Lakes connecting channels and harbors.

For the model tuning, however, it is desirable that field data corresponding to model output values be collected in the St. Marys River. These data include but are not necessarily limited to water velocities associated with ship passages in open water and under a modest variety of ice conditions.

Velocity data collection ideally would entail a current measurement program using self-recording current meters at one or two points on a given cross section. These devices obviate the need for making measurements on the ice under difficult and often hazardous conditions. A water sampling device affixed to the above mentioned current meter would provide a sample necessary to determine suspended-sediment concentration. Such an arrangement has been successfully employed in sediment transport studies near the Mississippi and Atchafalaya Deltas on the Louisiana coast. Sampling of the bed load would be necessary to determine sediment flux.

The sediment transport component of the model requires a knowledge of a number of sediment properties, all of which require a sediment collection program and laboratory analysis for their determination. The properties of interest include size distribution, settling velocity, and yield strength (for cohesive sediments). While some laboratory analyses are essential, a concurrent parameter or sensitivity study utilizing the numerical model significantly reduce the amount and nature of the laboratory work required.

A sensitivity analysis would be a valuable adjunct to the modeling work. A properly formulated test would obviate some of the work that would normally be undertaken as part of a calibration activity.

BIBLIOGRAPHY

Adams, C. E., Jr. and G. L. Weatherly, 1981. Suspended sediment transport and benthic boundary layer dynamics. Mar. Geol., 42, 1-18.

Bagnold, R. A., 1954. The Physics of Blown Sand and Desert Dunes. Methuen and Co., London, 265 p.

Blaauw, C. D. and H. A. Van de Kaa, 1978. Power and speed of push tows in canals. Proc., Symp. on Aspects of Navigability of Constrained Waterways, Delft, the Netherlands.

Gibbs, R. J., M. D. Matthews, and D. A. Link, 1971. The relationship between sphere size and settling velocity. Jour. Sed. Pet., 41, 7-18.

Hochstein, A., 1967. Navigation use of waterway canals.

----- 1981. Tennessee-Tombigbee supplemental environmental assessment. U.S. Army Corps of Engineers, Mobile District.

Hochstein, A. and C. E. Adams, Jr., 1985. An assessment of the effects of tow movements on the Kanawha River. Report to U.S. Army Corps of Engineers, Huntington District.

Hochstein, A. and M. Cohen, 1980. Interacton between tow traffic and channel. Proc. of Water Resources Forum, Houston, Texas.

Hodek, R. J., G. R. Alger, and H. S. Santeford, 1985. Development of a predictive model to assess the effects of extended season navigation on Great Lakes connecting waters, App. A, Site and soil conditions. Michigan Tech. Univ.

McCave, I. N., 1971. Sand waves in the North Sea off the coast of Holland. Mar. Geol., 10, 199-225.

Migniot, C., 1968. Etude des proprietes physiques de differents sediments tres fins et de leur comportement sous des actions hydrodynamiques. La Houille Blanche, 7, 591-620.

Miller, M. C., I. N. McCave, and P. D. Komar, 1977. Threshold of sediment motion under unidirectional currents. Sedimentology, 24, 507-527.

Smith, J. D., 1977. Modeling of sediment transport on continental shelves. In (E. D. Goldberg, I. N. McCave, J. J. O'Brien, and J. H. Steele, eds.) The Sea, Vol. 6, 539-577.

Smith, J. D. and S. R. McLean, 1977. Boundary layer adjustments to bottom topography and suspended sediment. In (J. C. J. Nihoul, ed.), Bottom Turbulence, Elsevier, New York, pp. 123-151.

Wiegel, R. L., 1964. Oceanographical Engineering. Prentice-Hall, Englewood Cliff, N.J., 532 p.

Wuebben, J. L., W. M. Brown, and L. J. Zabilansky, 1984. Analysis of physical effects of commercial vessel passage through the Great Lakes connecting channels. Cold Regions Research and Engineering Laboratory, 51 p. (+ tables and figures).

Yalin, M. S., 1963. An expression for bed load transportation. J. Hydraul. Div. Proc. Am. Soc. Civ. Eng., 89 (HY3), 221-250.